CT tube current for attenuation map in a combined PET/CT system: obese patient simulated phantom study

doi: 10.1007/s12149-012-0584-5

Title Page

Types of article: original article

CT tube current for attenuation map in a combined PET/CT system: obese patient simulated phantom study

Short title: CT tube current for PET image・Nagaki *et al.*

Akio Nagaki[1,2], Masahisa Onoguchi[2], Norikazu Matsutomo[1].

(1) Department of Radiological Technology, Kurashiki Central Hospital, Okayama, Japan

(2) Department of Health Sciences, Graduate School of Medical Sciences, Kanazawa University, Ishikawa, Japan

Corresponding author

Masahisa Onoguchi

Department of Health Sciences, Graduate School of Medical Sciences, Kanazawa University, Kodatsuno 5-11-80, Kanazawa, Ishikawa 920-0942, Japan

E-mail: onoguchi@staff.kanazawa-u.ac.jp

Phone & Fax: +81 76 265 2526

Abstract

Objective The CT portion of PET/CT provides attenuation correction of the PET emission scan. This study was performed to evaluate how much CT tube current can be lowered while still providing attenuation maps on PET images.

Methods Two body phantoms (outside diameters of 300 and 500 mm) were used to investigate and PET/CT acquisitions were performed with an Aquiduo PCA-7000B (Toshiba Medical Systems, Otawara, Japan). The CT scan was performed with the following parameters (120 kVp; 0.5-s rotation; 10, 20, 40, 80, 160, 200, 320, 460 mA). After the CT scan, PET images for ^{18}F- FDG (5.3 kBq/mL) were obtained for 4 min/bed position. The linear attenuation coefficients for ^{18}F-FDG in 300- and 500-mm phantoms, the pixel values and SD of CT images, the radioactivity concentration values and the hot- and cold-sphere contrast on PET images in the 500-mm phantom were evaluated.

Results In the 300-mm phantom, all eight tube currents gave of average linear attenuation coefficients of approximately 0.095 cm^{-1}. In contrast, the average linear attenuation coefficients of the 500-mm phantom at 10, 20, and 40 mA were significantly decreased (0.081, 0.087, and 0.092 cm^{-1}, respectively; $p < 0.05$) than 0.096 cm^{-1} of other tube currents. Further, CT pixel values decreased 10 and 20mA. Thus, the background radioactivity concentration values at 10 and 20 mA were substantially underestimated to

be 57% and 80%, respectively ($p < 0.05$); the hot-sphere contrast values at 10 and 20 mA were 0.26 and 0.29; the cold-sphere contrast values at 10, 20, and 40 mA were –0.33, –0.16, and 0.08.

Conclusions Although the linear attenuation coefficients in the 300-mm phantom remained the same with varying CT tube current, the 500-mm phantom yielded significant difference in the range 10–40mA. Therefore, the CT tube currents for attenuation correction should be adjusted over 40mA in obese patients.

Keywords: ^{18}F-FDG PET; CT tube current; attenuation map; PET/CT; obese patient.

Introduction

In recent years, a combined positron emission computed tomography-computed tomography (PET/CT) system has become increasingly clinical important as a functional and anatomical imaging modality [1–2]. The CT portion of combined PET/CT provides not only precise anatomical information to ^{18}F-fluorodeoxyglucose (^{18}F-FDG) imaging but also accurate attenuation correction of the PET emission scan [3]. The attenuation map generated from the CT scan will have several advantages in comparison with transmission scan requiring the use of radionuclide sources. The CT scan has much lower statistical noise and can be acquired much more quickly than a standard PET transmission scan. However, high X-ray tube current improve image quality but also increase radiation dose to the patient. Therefore, to reduce the radiation dose to the patient, the CT scan may be acquired at the optimal X-ray tube current for the purposes of diagnostic information, anatomical localization, and attenuation correction [4–6].

In obese patients, high photon attenuation and scatter deteriorate image quality of ^{18}F-FDG PET/CT, and PET acquisition protocols for obese patients have been reported [7, 8]. However, there have been few reports of CT-based attenuation

correction to improve PET image quality. The purpose of this study was to evaluate how much CT tube current can be lowered while still providing accurate attenuation maps on PET images in an obese patient simulated phantom.

Materials and methods

Phantom configuration

Three phantoms were used to evaluate image quality: Two body phantoms of different diameters (300-mm outer diameter × 180-mm length simulating normal torso, and 500-mm outer diameter × 180-mm length simulating obese torso) and a cylindrical scatter phantom (203-mm outer diameter × 700-mm length). 500mm outer diameter in the phantom corresponds to approximately 150 cm of abdominal circumference in human. Because the scan field of view of the CT scanner was 500-mm, we selected the 500-mm phantom as obese patients and expected maximum effect on CT tube current. Each body phantom contained a removable lung insert and six fill able spheres with internal diameters of 10, 13, 17, 22, 28, and 37 mm. The scatter phantom is a polyethylene cylinder, and a 6.4-mm hole is located off-axial at a radial distance of 45

mm and running parallel to the center axial of the cylinder into which an 800 mm-long plastic tube was inserted.

The phantom was filled with a solution of water and ^{18}F-FDG (5.3 kBq/mL) and the 4 smallest spheres with a radioactivity concentration 4 times that of the background based on NEMA standards [9]. The remaining 2 spheres (28, and 37 mm) were filled with air. To simulate the body activity from outside the scanner field of view (FOV), the scatter phantom was positioned at the edge of the body phantom. The plastic tube of the scatter phantom was filled with 116.6 Mbq of ^{18}F-FDG based on NEMA standards [9].

Data acquisition

A PET/CT scanner Aquiduo PCA-7000B combining a 16-multislice CT scanner with a high-resolution PET scanner was used (Toshiba Medical Systems, Otawara, Japan).

PET/CT examinations began with acquisition of a scout scan. After the definition of coaxial imaging range of the body phantom, CT images were obtained using the following parameters: 120 kVp, 0.5-s rotation, 2-mm slice thickness, 512 × 512 matrix size, and a table feed of 30 mm per rotation. The effect of the CT tube

current on the CT scan as an attenuation map was evaluated at eight tube currents: 10, 20, 40, 80, 160, 200, 320, and 460 mA. Thereafter, PET images were obtained in 3D mode for 4 min/bed position at 2-bed positions over the CT scan range. Eighty-one slices with a slice thickness of 2 mm were obtained for each bed position.

Image reconstruction

PET images were reconstructed into a 128 × 128 matrix with 1.34 zooming, using interactive algorithms (ordered-subset expectation maximization, 4 iterations, 14 subsets) and the CT-based attenuation map, and noise was reduced by smoothing the images with a 8-mm full width at half maximum (FWHM) Gaussian filter. The attenuation maps were calculated from CT images of 512 × 512 matrix by Aquiduo PCA-7000B software. The CT images were reduced to the 128 × 128 matrix of the PET images by a linear interpolation, and the CT pixel values in Hounsfield units (HU) were transformed into linear attenuation coefficients in cm^{-1} at 511 keV using the bilinear scaling method [10]. The attenuation maps were smoothed with Gaussian filter to make the resolution matched to the PET images. The CT images were acquired with eight tube currents (10, 20, 40, 80, 160, 200, 320, and 460 mA) on the PET/CT examination. The PET images were reconstructed eight images using one of the eight tube current settings for attenuation correction.

Image analysis

To compare with attenuation map in the 300- and 500-mm phantoms, the linear attenuation coefficients were measured in a pixel line on uniform slices without spheres and the average of 55 pixels in the 300-mm phantom and 90 pixels in the 500-mm phantom were calculated for comparison (Fig. 1a). The data of attenuation maps were exported to a personal computer and the files were converted raw ASCII with the software package XMedCon 0.9.9.0 (Ghent University, Ghent, Belgium).

The quantitative accuracy and the noise of the attenuation maps were assessed from the average and the standard deviation (SD) of CT pixel values in 16 regions of interest (ROIs) placed in the background on the central three slices of CT images with eight different tube currents (Fig. 1b). The quantitative accuracy and the noise of the PET images were evaluated from the average and the coefficient of variance (COV), the SD divided by the average, of radioactivity concentration values in the same background ROIs on CT images (Fig. 1c). In addition, the contrast on PET images was estimated from the hot- and cold-spheres as follows.

The hot-sphere (Q_H) = (C_{hot} — C_{bkgd}) / (C_{hot} + C_{bkgd})

The cold-sphere (Q_C) = (C_{bkgd} — C_{cold}) / (C_{bkgd} + C_{cold}),

where C_{bkgd}, C_{hot} and C_{cold} are the average radioactivity (Bq/mL) of all background ROIs (225 pixel), the hot-sphere 22-mm ROI (75 pixels) and the cold-sphere 37-mm ROI (225pixels). After the CT and PET images were transferred to a personal computer, placement and analysis of the ROIs and spheres on transaxial slices of the images were performed with the software package Prominence Processor Version 3.0 (Nihon Medi-Physics, Tokyo, Japan).

Analysis of variance (ANOVA) was used for multiple comparisons of the linear attenuation coefficient, CT pixel values, radioactivity and COV. ANOVA was performed by Tukey's method. In all analyses, $p < 0.05$ was considered to indicate statistical significance.

Results

Figure 2 shows representative the linear attenuation coefficients of two different tube currents at 10 and 460 mA in 300- and 500-mm phantoms by displaying horizontal profile curves. The two profile curves in 300-mm phantom were not apparently different, whereas the profile curve at 10mA was decreased in the central area than that at 460mA in 500-mm phantom. All of the average linear attenuation coefficients in the central area of the 300-mm phantom were approximately 0.095 cm^{-1}.

In the 500-mm phantom, the average linear attenuation coefficients at 10, 20, and 40 mA were significantly decreased (0.081, 0.087, and 0.092 cm^{-1}, respectively; $p < 0.05$) than 0.095 cm^{-1} or 0.096 cm^{-1} at over 80 mA (Table 1).

We evaluated effect of varying CT tube current for the CT images and the PET images in the 500-mm phantom. The CT pixel values at 10 and 20 mA were significantly decreased (–148.1 and –64.9, respectively; $p < 0.05$) than approximately –6.2 at over 80 mA (Fig. 3a). The trend of the SD of CT pixel values decreasing was observed increasing CT tube current (Fig. 3b). The background radioactivity concentration values at 10 and 20 mA were substantially underestimated to be 57% and 80%, respectively, and showed significantly decreased ($p < 0.05$) than those at over 40 mA (Fig. 4a). However, the background radioactivity concentration values were almost constant over the ranged from 80 to 460mA. The COV in PET images was not a significantly different except at 10 and 460 mA (19.4% and 16.1%, respectively; $p < 0.05$) (Fig. 4b). The hot-sphere contrast values at 10 and 20 mA were 0.17 and 0.22, respectively, which were decreased than the values of 0.30, 0.33, 0.33, 0.33, 0.33, and 0.28 for40, 80, 160, 200, 320 and 460 mA, respectively (Fig. 5a). The cold-sphere contrast values at 10, 20, and 40 mA were –0.31, –0.13, and 0.13, respectively, and were decreased than those of 0.32, 0.33, 0.32, 0.31, and 0.36 for 80, 160, 200, 320, and 460

mA, respectively (Fig. 5b). A declining trend in the hot- and cold-sphere contrast values versus tube current were observed under 40mA. In particular, the cold-sphere contrast at 10 and 20 mA showed negative values and the cold-sphere count was higher than the background count.

Figure 6 shows transverse image slices thought the plane of spheres in the 500-mm phantom for CT scans, attenuation maps, and PET scans at eight tube currents with the same window and level. The image of CT scan at 10 mA showed low contrast and noisy compared with 460 mA, and the attenuation map showed low contrast imaging. Thus, the PET images were undercorrected, and the cold-sphere lesion yielded radioactivity concentration. However, attenuation maps and PET images at over 80 mA were almost similar in contrast and background noise, and at 40 mA were slightly deteriorated.

Discussion

This study was performed to evaluate how much CT tube current can be lowered while still providing accurate attenuation maps on PET images using two body phantoms of different diameters. We showed here that the linear attenuation coefficients

in the 300- mm phantom had the same value at all of varying CT tube current examined, and the linear attenuation coefficient of central area and CT pixel values in the 500- mm phantom yield the significantly decrease at low CT tube currents in the range 10–40mA. These inaccurate corrections were not affect the COV in PET images, but caused loss of radioactivity concentration values and deterioration contrast on PET images.

A combined PET/CT system allows CT and PET images to be obtained in a single examination but also increases radiation dose to the patient. If a PET-only examination is required or serial studies are necessary in the same patient, the CT scan can be used at very low tube current for attenuation correction only [5]. In contrast, although higher CT tube current is required to produce diagnostic CT scans, a fixed CT tube current at 80 mA may be used to reduce the radiation dose to patients [11, 12]. Kamel *et al.* [13] reported that the CT tube current can be reduced while still yielding adequate attenuation correction of PET scans, and CT tube currents in the range 10–120mA yielded the same values for FDG uptake or lesion size. Therefore, they showed that the very low CT tube current is sufficient if the CT scan is only used for attenuation correction. Our findings were consistent with these results in the 300- mm normal weight patient simulated phantom, because of the linear attenuation coefficients

were not substantially different at all varying CT tube currents. However, the linear attenuation coefficients in the range 10–40mA yielded significant differences in the 500- mm obese patient simulated phantom. These finding indicated that an error in line attenuation coefficients in CT-based attenuation correction were most likely to have been caused by the much larger phantom size and a variety of CT scan-specific parameters [13, 14], such as tube voltage (kVp), tube current (mA) and rotation time (s). Fahey *et al.* [15] evaluated dosimetry and the combination of both lower CT tube voltage and tube current for adequate CT-based attenuation correction for PET in pediatric patients, and CT acquisition parameters were shown to be adequate for pediatric but not for adult patients. Thus, although the use of a cylindrical phantom (200 mm in diameter and length) and a torso phantom (anteroposterior thickness of 280 mm and lateral thickness of 380 mm) allow to evaluation in patient of normal weight, these results may not be comparable to reported adequate CT tube current in obese patient.

Our data indicate that PET images in the central area of the 500-mm phantom were undercorrected at very low CT tube currents. CT images offer improved contrast, resolution, and noise characteristics in comparison with transmission images obtained with radionuclide sources [16]. Although CT scan reduces statistical noise at high photon flux, the X-ray beam from 30 to 140 keV has a polychromatic spectram [17] and

much lower effective energy than the ^{68}Ge-^{68}Ga radionuclide sources from 511 keV. In PET imaging, the photon flux is much more attenuated by soft tissue absorption in obese patients compared to patients of normal weight. Similarly in the CT imaging, the CT pixel values were decreased and CT images were noisy at 10 and 20mA. Furthermore, low CT pixel value worsened attenuation maps. Thus, the radioactivity concentration values, the hot- and cold-sphere contrast at 10–40 mA were decreased at over 80 mA. This finding should be noted as it indicates that the very low tube current in obese patients varied the quantified uptake values, such as standardized uptake values (SUV), which are of clinical importance for management of cancer patients [18]. However, because of the attenuation maps were reduced matrix size and smoothed with Gaussian filter, the SD of CT pixel values were few different the COV of PET images except at 10 and 460mA.

This study was limited to the use of one type of PET/CT scanner and therefore the result may not be applicable to other PET/CT scanners. The tube currents and tube voltages may differ between PET/CT scanner manufactures due to differences in beam filtration, beam-shaping filters, geometry, and acquisition algorithms, *etc*. Furthermore, this investigation did not consider the clinical whole-body data in obese patients.

Conclusion

We examined the CT tube current for the attenuation maps using two body phantoms of different diameter. Although the linear attenuation coefficients in the 300-mm phantom remained the same with varying CT tube current, the 500-mm phantom yielded significant difference in the range 10–40mA. Therefore, the CT tube currents for attenuation correction should be adjusted over 40mA in obese patients. These findings indicate that radioactivity concentration values and contrast on PET images may be adversely affected at very low CT tube currents on PET/CT examination in obese patients.

Acknowledgement

The authors thank Dr Keiichi Matsumoto (Department of Radiological Technology, Faculty of Medical Science, Kyoto College of Medical Science) for providing the 500-mm phantom.

References

1. Cohade C, Wahl RL. Applications of positron emission tomography/computed tomography image fusion in clinical positron emission tomography-clinical use, interpretation methods, diagnostic improvements. *Semin Nucl Med.* 2003;33:228-37.

2. Schöder H, Yeung HW, Larson SM. CT in PET/CT: essential features of interpretation. *J Nucl Med.* 2005;46:1249-51.

3.Townsend DW. Dual-modality imaging: combining anatomy and function. *J Nucl Med.* 2008;49:938-55.

4. Wu TH, Huang YH, Lee JJ, Wang SY, Wang SC, Su CT, *et al.* Radiation exposure during transmission measurements: comparison between CT- and germanium-based techniques with a current PET scanner. *Eur J Nucl Med Mol Imaging.* 2004;31:38-43.

5. Wu TH, Chu TC, Huang YH, Chen LK, Mok SP, Lee JK, *et al.* A positron emission tomography/computed tomography (PET/CT) acquisition protocol for CT radiation dose optimization. *Nucl Med Commun.* 2005;26:323-30.

6. Brix G, Lechel U, Glatting G, Ziegler SI, Münzing W, Müller SP, *et al.* Radiation exposure of patients undergoing whole-body dual-modality 18F-FDG PET/CT examinations. *J Nucl Med.* 2005;46:608-13.

7. Halpern BS, Dahlbom M, Auerbach MA, Schiepers C, Fueger BJ, Weber WA, *et al.*

Optimizing imaging protocols for overweight and obese patients: a lutetium orthosilicate PET/CT study. *J Nucl Med*. 2005;46:603–607.

8. Masuda Y, Kondo C, Matsuo Y, Uetani M, Kusakabe K. Comparison of Imaging Protocols for ^{18}F-FDG PET/CT in Overweight Patients: Optimizing Scan Duration Versus Administered Dose. *J Nucl Med*. 2009;50:844–848.

9. National Electrical Manufacturers Association. *NEMA Standards Publication NU 2-2001: Performance Measurements of Positron Emission Tomographs.* Rosslyn, VA: National Electrical Manufacturers Association; 2001.

10. Townsend DW. Positron emission tomography/computed tomography. *Semin Nucl Med*. 2008;38:152-66.

11. Coleman RE, Delbeke D, Guiberteau MJ, Conti PS, Royal HD, Weinreb JC, *et al.* American College of Radiology; Society of Nuclear Medicine; Society of Computed Body Tomography and Magnetic Resonance. Concurrent PET/CT with an integrated imaging system: intersociety dialogue from the joint working group of the American College of Radiology, the Society of Nuclear Medicine, and the Society of Computed Body Tomography and Magnetic Resonance. *J Nucl Med.* 2005;46:1225-39.

12. Hany TF, Steinert HC, Goerres GW, Buck A, von Schulthess GK. PET diagnostic accuracy: improvement with in-line PET-CT system: initial results. *Radiology.*

2002 ;225:575-81.

13. Kamel E, Hany TF, Burger C, Treyer V, Lonn AH, von Schulthess GK, *et al.* CT vs 68Ge attenuation correction in a combined PET/CT system: evaluation of the effect of lowering the CT tube current. Eur J Nucl Med Mol Imaging. 2002;29:346-50.

14. Reza Ay M, Zaidi H. Computed tomography-based attenuation correction in neurological positron emission tomography: evaluation of the effect of the X-ray tube voltage on quantitative analysis. *Nucl Med Commun.* 2006;27:339-46.

15. Fahey FH, Palmer MR, Strauss KJ, Zimmerman RE, Badawi RD, Treves ST. Dosimetry and adequacy of CT-based attenuation correction for pediatric PET: phantom study. *Radiology.* 2007;243:96-104.

16. Nakamoto Y, Osman M, Cohade C, Marshall LT, Links JM, Kohlmyer S, *et al.* PET/CT: comparison of quantitative tracer uptake between germanium and CT transmission attenuation-corrected images. *J Nucl Med.* 2002;43:1137-4.

17. Beyer T, Townsend DW, Brun T, Kinahan PE, Charron M, Roddy R, *et al.* A combined PET/CT scanner for clinical oncology. *J Nucl Med.* 2000;41:1369-1379.

18. Thie JA. Understanding the standardized uptake value, its methods, and implications for usage. *J Nucl Med.* 2004;45:1431-4.

Figure Legends

Fig. 1 Datasets of 500-mm phantom for analysis. The linear attenuation coefficient was measured in a pixel line on uniform slices (a). Circular ROIs placed over the CT images and the PET images. We evaluated the HU and SD of CT pixel values (b), the COV of background radioactivity concentration values (c) and the hot- and cold-sphere contrast (d).

Fig. 2 The profile curves of linear attenuation coefficients at 10mA and 460mA measured in attenuation maps of 300-mm phantom (a) and 500-mm phantom (b).

Fig. 3 Average pixel values (a) and SD of pixel values for CT images divided according to CT tube current settings (b). *Statistically significant difference, $p<0.05$ to 20, 40, 80, 160, 200, 320 and 460mA; **$p<0.05$ to 40, 80, 160, 200, 320 and 460mA.

Fig. 4 Average background radioactivity concentration values (a) and COV for PET images divided according to CT tube current settings (b). *Statistically significant difference, $p<0.05$ to 20, 40, 80, 160, 200, 320 and 460mA; **$p<0.05$ to 40, 80, 160,

200, 320 and 460mA; ***p<0.05 to 460mA.

Fig. 5 Contrast in hot-sphere (a), and cold-sphere (b) for acquired PET images divided according to CT tube current settings.

Fig. 6 CT images, attenuation maps, and PET images for different CT tube current settings.

Table 1

Average linear attenuation coefficients in center area

Tube current (mA)	300-mm phantom (cm^{-1})	500-mm phantom (cm^{-1})
10	0.095	0.081 *
20	0.095	0.087 *
40	0.095	0.092 *
80	0.095	0.095
160	0.095	0.096
200	0.095	0.096
200	0.095	0.096
320	0.095	0.096
460	0.095	0.096

* $p < 0.05$ when compared with over 80 mA linear attenuation coefficients.

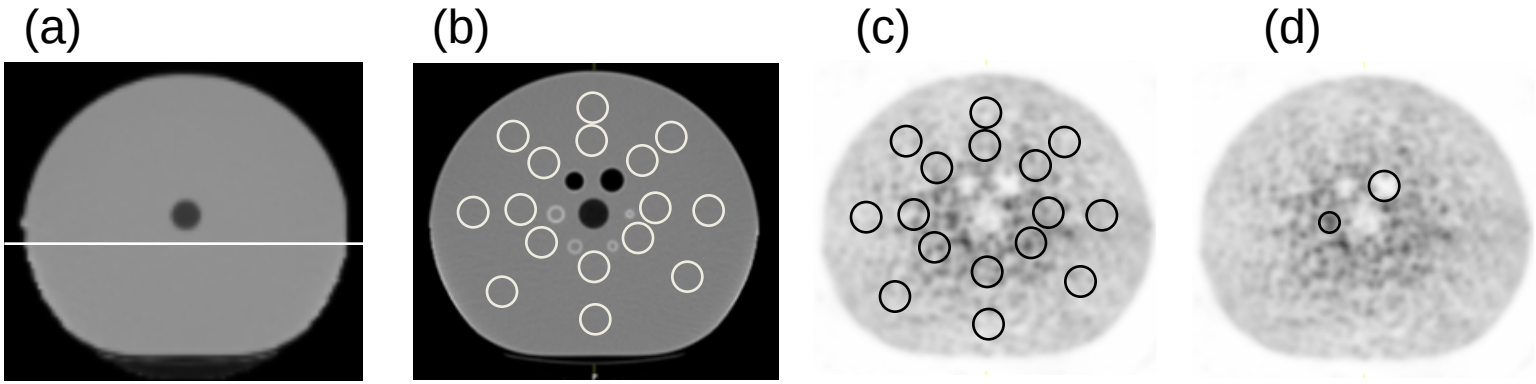

Fig. 1

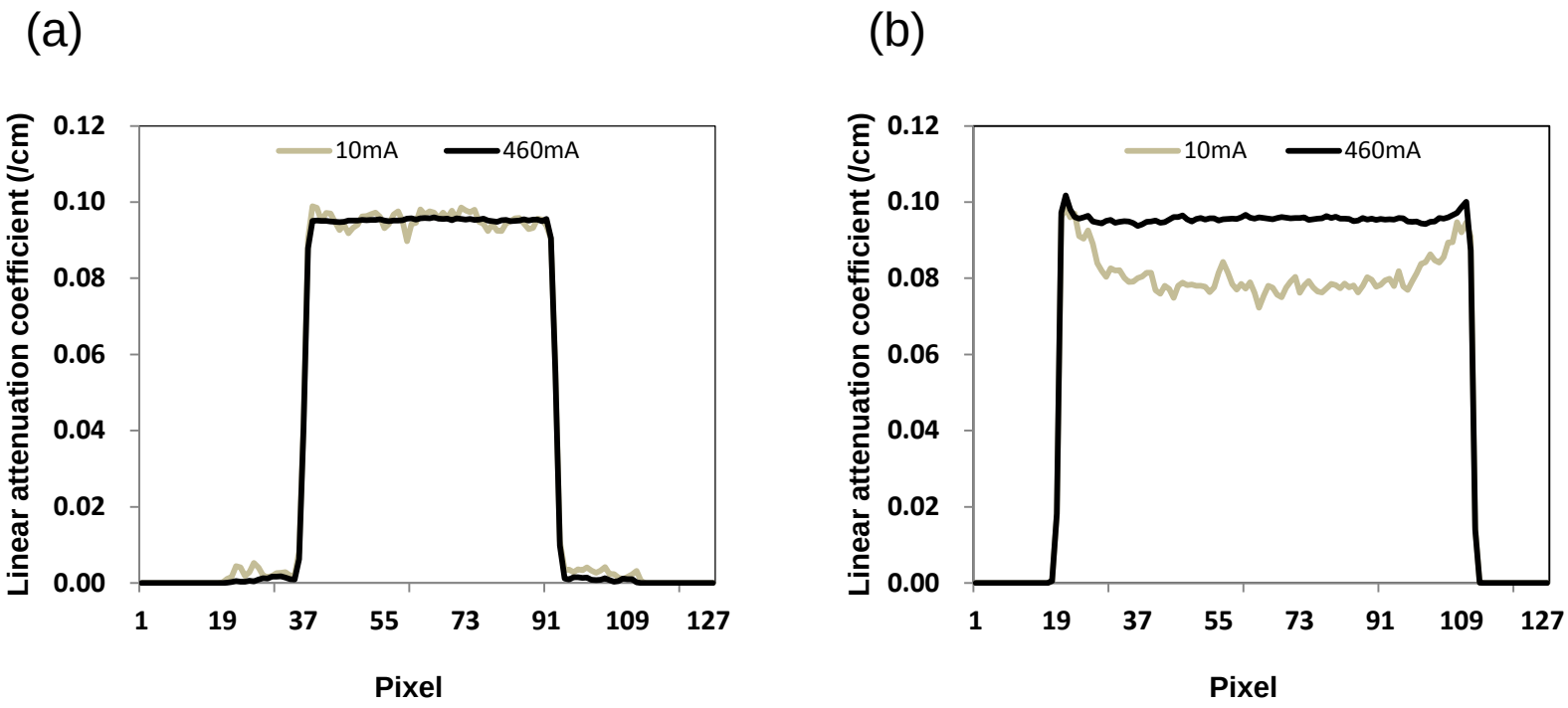
(a)
(b)
Linear attenuation coefficient (/cm)
0.12
0.10
0.08
0.06
0.04
0.02
0.00
10mA
460mA
1
19
37
55
73
91
109
127
Pixel

Fig. 2

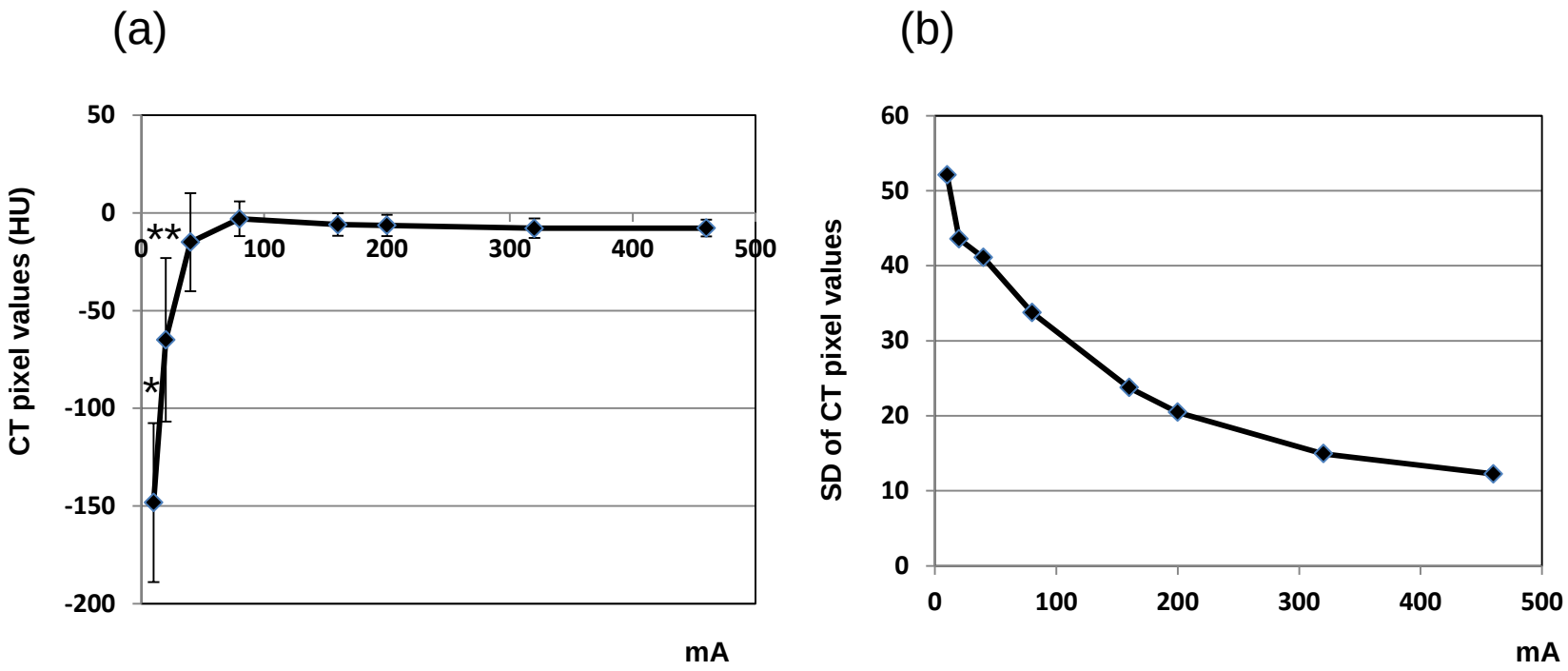
(a)
CT pixel values (HU)
50
0
-50
-100
-150
-200
0
100
200
300
400
500
**
*
mA
(b)
SD of CT pixel values
60
50
40
30
20
10
0
0
100
200
300
400
500
mA

Fig. 3

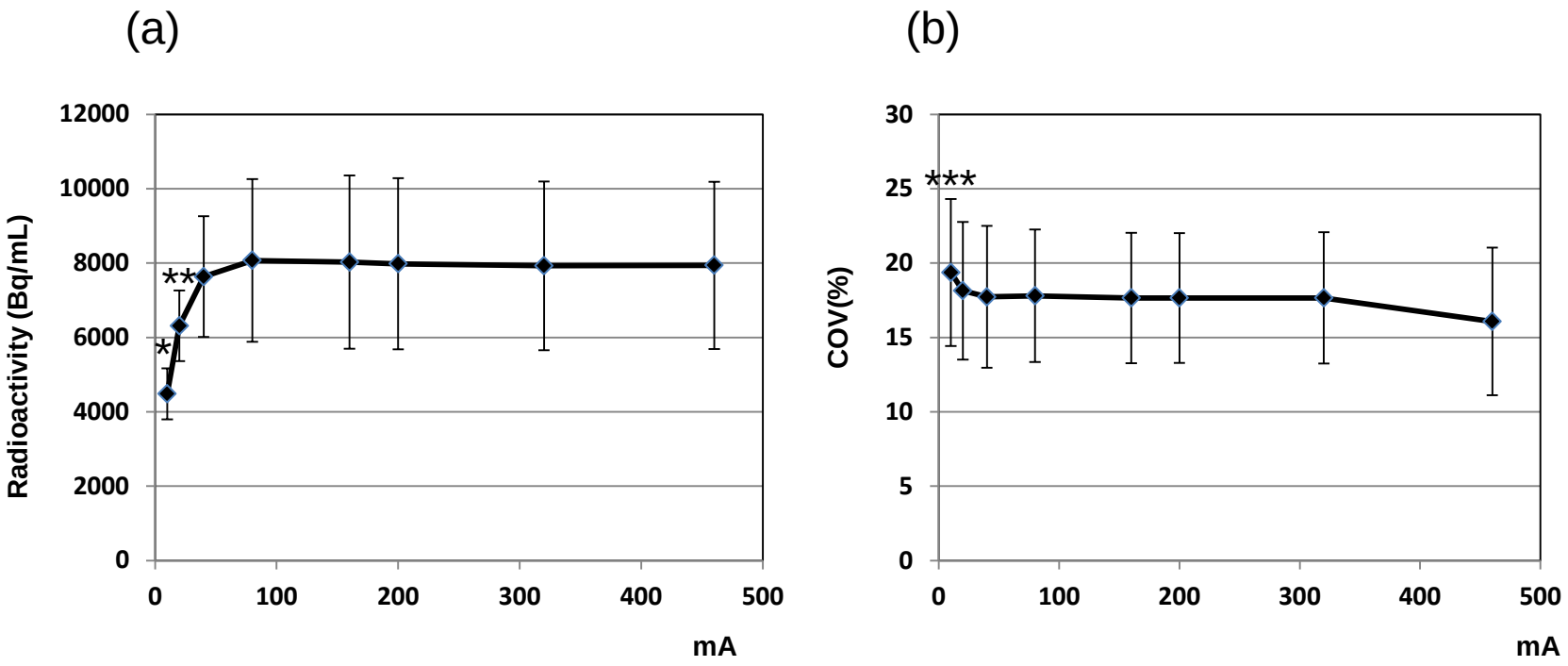
(a)
Radioactivity (Bq/mL)
12000
10000
8000
6000
4000
2000
0
*
**
0
100
200
300
400
500
mA
(b)
COV(%)
30
25
20
15
10
5
0
***
0
100
200
300
400
500
mA

Fig. 4

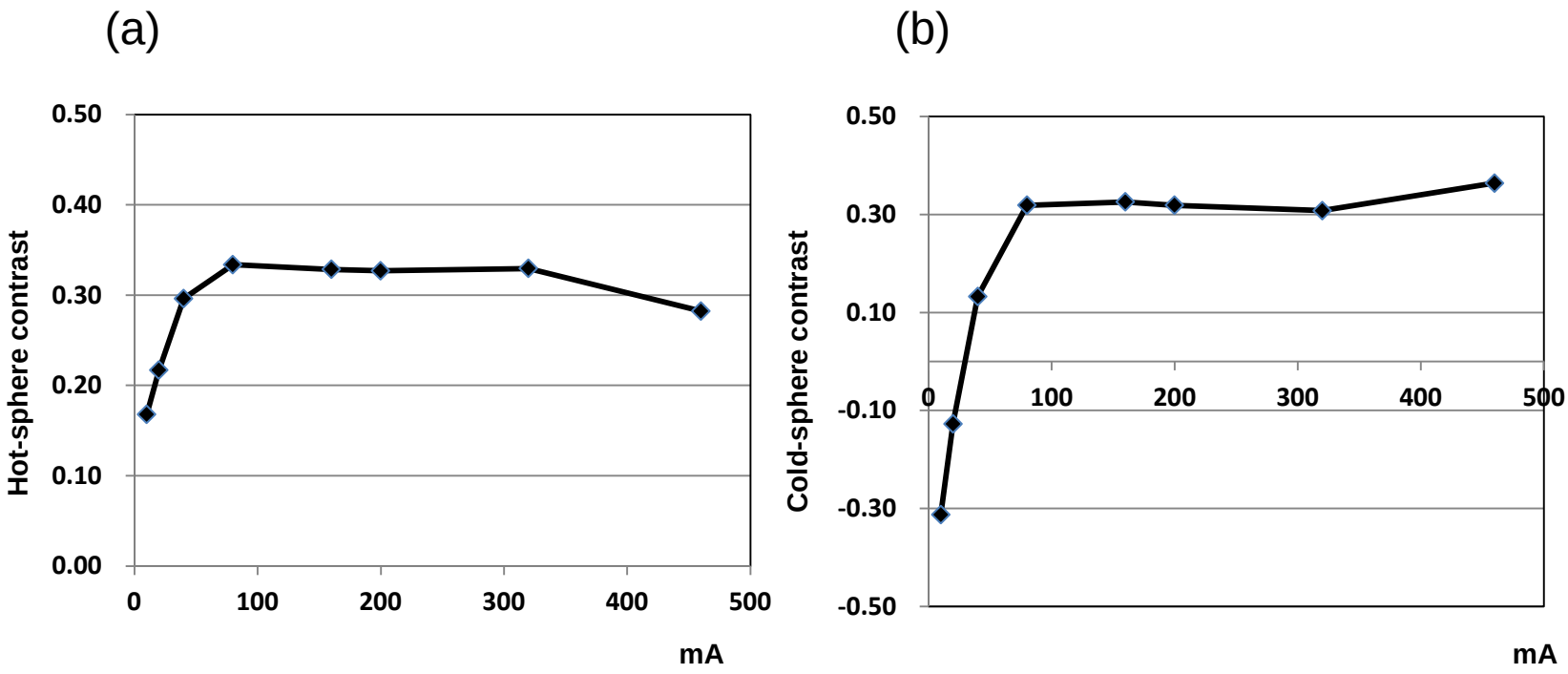
(a)
(b)
Hot-sphere contrast
0.50
0.40
0.30
0.20
0.10
0.00
0
100
200
300
400
500
mA
Cold-sphere contrast
0.50
0.30
0.10
-0.10
-0.30
-0.50
0
100
200
300
400
500
mA

Fig. 5

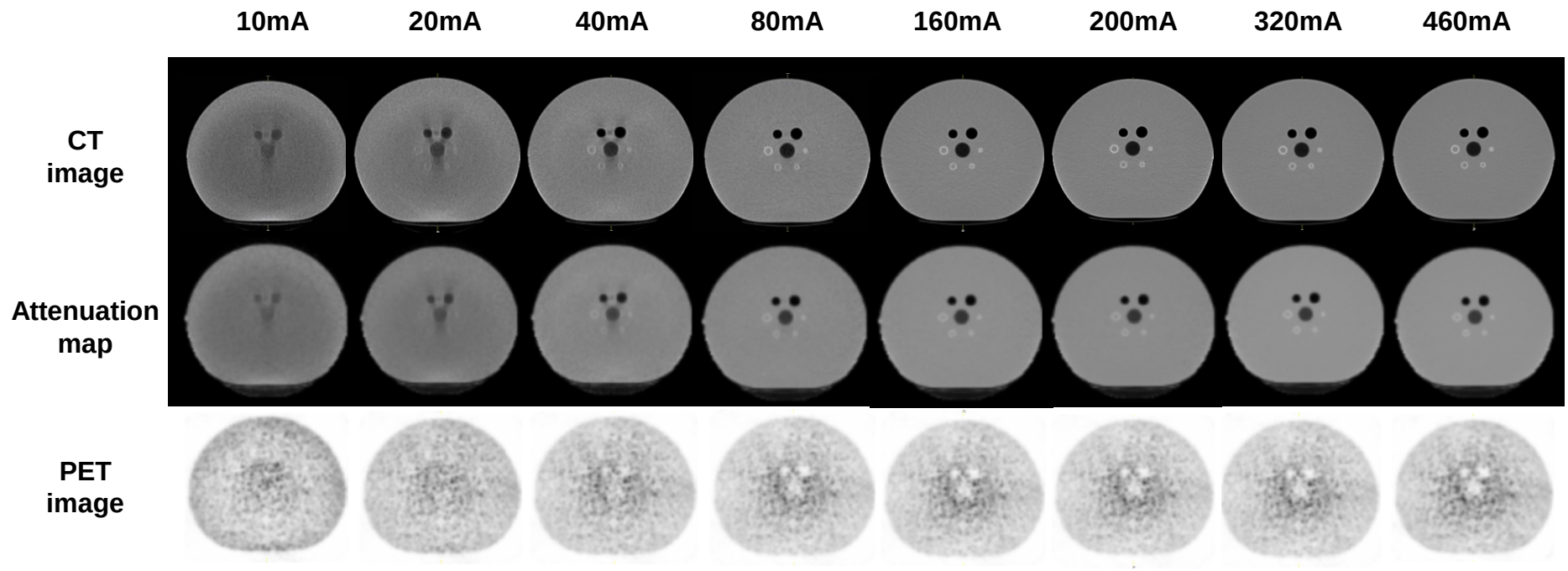
10mA
20mA
40mA
80mA
160mA
200mA
320mA
460mA
CT image
Attenuation map
PET image

Fig. 6